Reactions of Laser-Ablated Boron Atoms with Methylamines. Matrix Infrared Spectra and MP2 Frequency Calculations for Isotopic Product Molecules

Dominick V. Lanzisera and Lester Andrews*

Department of Chemistry, University of Virginia, Charlottesville, Virginia 22901

Received: September 10, 1996; In Final Form: November 11, 1996[⊗]

Reactions of laser-ablated boron atoms with monomethylamine in argon produce two new iminoboranes, CH_3BNH and CH_3NBH, as well as the related isomer, CH_2BNH_2. Boron reactions with dimethylamine also generate these products and a third new iminoborane, CH_3BNCH_3. These molecules are identified by matching observed matrix infrared and MP2 calculated $^{10}B/^{11}B$ isotopic frequency ratios. In these reactions, the observed products indicate that the primary reaction mechanisms involve boron insertion into either the C−N or N−H bonds, instead of into the C−H bonds.

Introduction

High-energy molecules which are reactive at room temperature can often be preserved at cryogenic temperatures. For several years, matrix isolation spectroscopy has enabled the study of otherwise reactive species, including products containing boron.[1−5] Because of the low vapor pressure of boron at all but extremely high temperatures, laser ablation is a convenient way to produce atomized boron to form new reaction products. In addition, laser-ablated boron atoms possess excess kinetic energy which increases the reaction probability and facilitated the study of reactions of boron with small molecules such as O_2, N_2, H_2O, and H_2 in argon matrices.[1−5] For reactions with polyatomic gases, such as CH_4[6,7] and NH_3,[8,9] matrix isolation enabled the production and retention of several novel compounds. In these two experiments, the primary mechanisms involved insertion into a C−H or N−H bond followed by dehydrogenation. Because the energy of the C−H bond in methane exceeds that of the N−H bond in ammonia, boron reactions with NH_3 yielded more product. In the experiments reported here, boron reacts with monomethylamine, CH_3NH_2, a molecule that possesses C−H and N−H bonds as well as a C−N bond. The reaction of boron with dimethylamine, $(CH_3)_2$-NH, complements the monomethylamine work. The results of these studies should allow one to assess the relative proficiencies of each of three insertion mechanisms.

Because of their similarity to alkynes, iminoboranes are some of the more interesting boron compounds. Three groups[9−11] have characterized HBNH, and this molecule has been isolated in a matrix following the reaction of laser-ablated boron with ammonia.[8,9] In this article, we describe boron atom reactions with mono- and dimethylamine. Infrared spectra of reactive species isolated in an argon matrix enables the identification of novel products. Ab initio calculations of the energies, structures, and vibrational frequencies of several potential product species facilitate this identification. The observed products provide insights into the mechanisms of boron insertion reactions.

Experimental Section

Previous articles have described the apparatus for pulsed laser ablation, matrix isolation, and FTIR spectroscopy;[1,2] an APD Cryogenics 6.5 K refrigerator was used here. Mixtures of 1% CH_3NH_2 or $(CH_3)_2NH$ in Ar codeposited at 3 mmol/h for 3 h onto a 6−7 K cesium iodide window react with boron atoms ablated from a target source rotating at 1 rpm. The fundamental 1064 nm beam of a Nd:YAG laser (Spectra Physics DCR-11) operating at 10 Hz and focused with a $f = +20$ cm lens ablated the target using 30 mJ per 10 ns pulse. Reagent gases included CH_3NH_2 and $(CH_3)_2NH$ (both from Matheson) and CH_3ND_2 (MSD Isotopes). We employed three samples of boron: ^{nat}B (Aldrich, 80.4% ^{11}B, 19.6% ^{10}B), ^{10}B (93.8%, Eagle Pitcher Industries), and ^{11}B (97.5%, Eagle Pitcher Industries). Following deposition, a Nicolet 550 Fourier transform infrared (FTIR) spectrometer collected infrared spectra using a liquid nitrogen cooled MCT detector. The resolution of these spectra was 0.5 cm^{-1} with an accuracy of ± 0.2 cm^{-1}. After sample deposition, annealing to 15 K followed by broad band mercury arc photolysis (Philips 175 W) produced changes in the FTIR spectra. Further annealings to 25 and 35 K also changed some of the spectral features.

We performed Hartree−Fock (HF) calculations on potential product molecules using the Gaussian 94 program package.[12] For all calculations, a Møller−Plesset correlation energy correction followed the HF calculation and was truncated at second order (MP2 method).[13] The basis set for each atom was the Dunning/Huzinaga full double ζ with one single first polarization function (D95*).[14] The geometry optimizations used redundant internal coordinates and converged via the Berny optimization algorithm,[12,15] and the program calculated vibrational frequencies analytically.

Results

Infrared spectra of the reaction products of methylamines with boron using various isotopic combinations are reported. Several strong absorptions show no boron isotopic shift and typically correspond to either the precursor or fragments of the precursor created by photochemistry from the laser plume. For example, in each spectrum with CH_3NH_2, peaks at 1640, 1452, 1346, 1123, 1064, and 1059 cm^{-1} corresponding to CH_2NH and at 3615.9, 2027.8, and 478.4 cm^{-1} due to HNC were observed.[16,17] Also detected were HCN absorptions at 3305.1, 2093.4, and 721.4 cm^{-1}, the CN absorption at 2044 cm^{-1},[17,18] and at most extremely weak CH_4 and CH_3 absorptions near 1304 and 610 cm^{-1}, respectively.[19] In the $(CH_3)_2NH$ experiments, several CH_2NCH_3 absorptions were observed.[20] The remainder of this section deals only with new species containing boron. In addition to the new absorptions reported below, peaks corresponding to HBO, BO, BO_2, $(BO)_2$, and BO_2^- were observed because of oxides on the surface of the boron target.[1,2]

[⊗] Abstract published in *Advance ACS Abstracts,* January 1, 1997.

S1089-5639(96)02772-7 CCC: $14.00

TABLE 1: Frequencies (cm^{-1}), Photolysis Behavior, and Identity of Product Species in the B + CH_3NH_2 Experiments

10/1[a]	11/1[a]	10/2[a]	11/2[a]	photolysis[b]	identity
3712.3	3710.6			+35	HBNH
3702.1	3701.6	2794.4	2789.6	+35	HBNH
3691.1	3690.5			+40	CH_3BNH
2307.6	2298.3			+15	$(H_2)BH$
2268.6	2259.3	1695.2	1682.8	0	BH
2171.5	2170.8	2171.5	2171.8	−40	BCN
2094.3	2092.2	2094.3	2092.2	+60	BH_2CN
2068.1	2055.1	2068.1	2055.1	+5	BNC
2020.6	1981.1	2020.6	1981.1	+15	CH_3NB
2001.2	1940.2	1950.7	1892.2	+40	CH_3BNH
1975.5	1949.2	1753.5	1749.2	+20	CH_3NBH
1939.3	1881.0	1895.3	1839.4	+30	CH_2BNH
1880.0	1829.6			−80	BNH
1876.4	1846.2	1729.0	1717.6	+5	BNBH
1836.4	1830.5	1836.4	1830.5	−30	CH_2NB
1825.7	1788.1	1768.9[c]	1732.3[c]	+35	HBNH
1819.7	1782.7	1616.2		+35	HBNH
1798.5	1743.5	1794.1[d]	1741.1[d]	−10	CH_2BNH_2
1769.1	1736.4	1769.1	1736.4	−70	BNB
1556.5	1533.2			−100	BNH_2
1514.4	1504.6			−100	?
1016.6	984.3	1016.6	984.3	+5	BNC
901.5		901.5		+10	B_2N
826.2	800.1	826.2	800.1	−40	BCN
464.8	463.5			+35	HBNH

[a] The first number is the mass number of the boron isotope, and the second number is the mass number of the hydrogen isotope. [b] Percent change of peak intensity following 30 min of broad band mercury arc photolysis. [c] Peaks listed are for the mixed isotopic molecule, HBND. [d] Peaks listed are for those of the mixed isotopic molecule CH_2BNHD. CH_2BND_2 absorptions occur at 1786.2 and 1734.8 cm^{-1} for ^{10}B and ^{11}B, respectively.

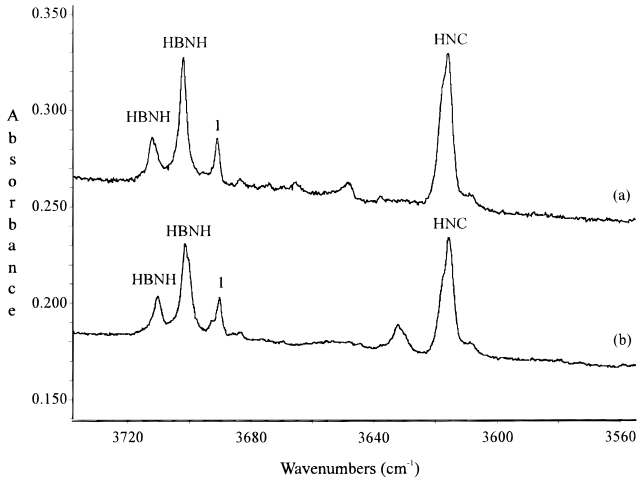

Figure 1. Infrared spectra in the 3740−3560 cm^{-1} N−H stretching region following pulsed laser ablation of B atoms codeposited with Ar/CH_3NH_2 samples on a CsI window at 6−7 K: (a) ^{10}B + CH_3NH_2 and (b) ^{nat}B + CH_3NH_2. Numbers above peaks refer to assignments of new products described in the text.

^{10}B + CH_3NH_2. Table 1 provides frequencies and photolysis behavior of all isotopic combinations of boron−monomethylamine reactions. Figure 1a displays a spectrum for the best ^{10}B experiment in the N−H stretching region. The strong bands at 3712.3 and 3702.1 cm^{-1}, observed previously in the reactions of boron with ammonia, correspond to HBNH,[8,9] and the 3615.9 cm^{-1} band is due to HNC. A new absorption appears at 3691.1 cm^{-1} and increases 40% upon photolysis.

The B−N stretching region of the spectrum (Figure 2a) contains many product peaks. HBNH absorptions at 1825.7 and 1819.7 cm^{-1}, the BNBH absorption at 1876.4 cm^{-1}, the BNH absorption at 1880.0 cm^{-1}, and the BNB absorption at

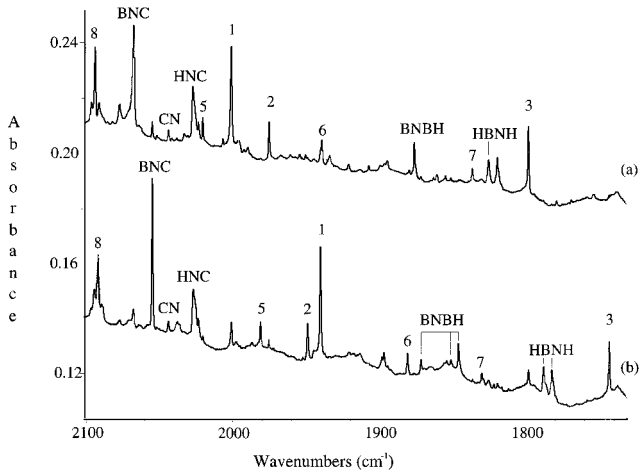

Figure 2. Infrared spectra in the 2100−1740 cm^{-1} B−N stretching region following pulsed laser ablation of B atoms codeposited with Ar/CH_3NH_2 samples on a CsI window at 6−7 K: (a) ^{10}B + CH_3NH_2 and (b) ^{nat}B + CH_3NH_2. Numbers above peaks refer to assignments of new products described in the text.

1769.1 cm^{-1} agree with the ammonia experiments.[8,9] Peaks due to BCN at 2171.5 cm^{-1} and BNC at 2068.1 cm^{-1} match those from a parallel study of B + HCN reactions.[21] Among the new peaks, a strong absorption at 2001.2 cm^{-1} increases 40% on photolysis, a sharp absorption at 2094.3 cm^{-1} increases 60%, and another absorption at 1975.5 cm^{-1} increases 20%. By contrast, a strong, sharp absorption at 1798.5 cm^{-1} decreases 10% following photolysis, and a small absorption at 1836.4 cm^{-1} decreases 30%. In the bending region, new absorptions at 1016.6 and 826.2 cm^{-1} correspond to BNC and BCN, respectively.[20] A sharp peak at 464.8 cm^{-1} is due to HBNH.

^{nat}B + CH_3NH_2. Figure 1b presents a spectrum in the N−H stretching region for the best natural boron experiment. Because the vibrational modes in this region involve mainly nitrogen and hydrogen, small boron isotopic shifts are expected. The strong bands at 3710.6 and 3701.6 cm^{-1} track with the 3712.3 cm^{-1} and 3702.1 cm^{-1} bands from the ^{10}B experiment and correspond to HBNH.[8,9] A new absorption appears at 3690.5 cm^{-1}, and this peak increases 40% upon photolysis, thereby tracking with the nearby 3691.1 cm^{-1} band from the ^{10}B experiment.

In the B−N stretching region (Figure 2b), the above ^{10}B absorptions were observed along with displaced ^{11}B counterparts. HBNH absorptions at 1788.1 and 1782.7 cm^{-1} appear in the ammonia experiment, as does the BNBH isotopic quartet at 1876.4, 1871.4, 1851.5, and 1846.2 cm^{-1}. A strong BNC band at 2055.1 cm^{-1} accompanies a smaller BCN peak at 2170.8 cm^{-1}. Among the new peaks, a strong absorption at 1940.2 cm^{-1} increases 40% on photolysis and has a counterpart approximately one-fourth the size at 2001.2 cm^{-1} with the same photolysis behavior as in the ^{10}B experiment; these two peaks, then, correspond to the same single-boron species. The ^{10}B experiment absorption at 1975.5 cm^{-1} similarly tracks with the ^{nat}B peak at 1949.2 cm^{-1} (both +20% on photolysis). In addition, a peak at 1743.5 cm^{-1} exhibits a 4:1 doublet with a peak at 1798.5 cm^{-1}, and both peaks decrease 10% on photolysis. Table 1 lists other ^{11}B absorptions with their ^{10}B counterparts.

^{11}B + CH_3NH_2. Experiments performed with ^{11}B confirm the identification of product absorptions from the ^{10}B and ^{nat}B experiments because bands absent in ^{11}B experiments must arise from ^{10}B species. No new absorptions appeared, as expected, and the spectrum is not shown here.

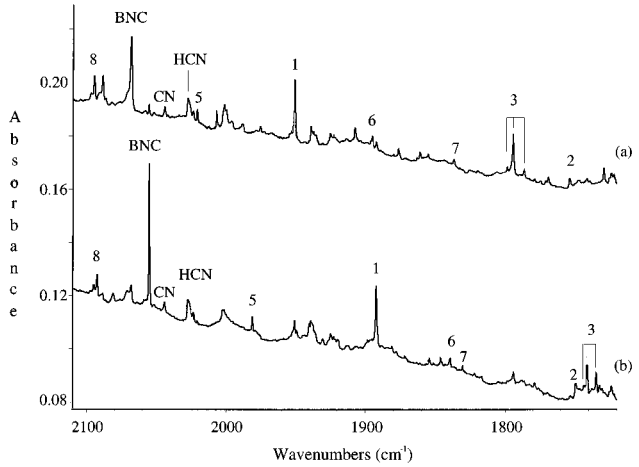

Figure 3. Infrared spectra in the 2110−1730 cm^{-1} B−N stretching region following pulsed laser ablation of B atoms codeposited with Ar/CH_3ND_2 samples on a CsI window at 6−7 K. (a) $^{10}B + CH_3ND_2$ and (b) $^{nat}B + CH_3ND_2$. Numbers above peaks refer to assignments of new products described in the text.

$^{10}B + CH_3ND_2$. Because of hydrogen exchange on the amine group, experiments were performed with successively increased deuteration. This enrichment with the mixed precursors, CH_3NH_2, CH_3NHD, and CH_3ND_2, actually served as an advantage because it allowed for the observation of isotopic multiplets with changing relative intensities as a function of deuterium enrichment. In the B−N stretching region (Figure 3a), a strong new absorption at 1950.7 cm^{-1} increases 40% upon photolysis. Another prominent peak at 1794.1 cm^{-1} decreases 10% upon photolysis. A nearby peak of lower intensity at 1786.2 cm^{-1} also decreases 10% upon photolysis, and the proximity of these two absorptions to the 1798.5 cm^{-1} peak from CH_3NH_2 experiments indicates that these three peaks form a triplet and, therefore, correspond to a species with two amine hydrogens, whereas the 1950.7 cm^{-1} peak forms a doublet with the hydrogen component at 2001.2 cm^{-1}, denoting a single amine hydrogen. Table 1 lists other absorptions from deuterated products. Noteworthy is that, of the new absorptions observed in the $^{10}B + CH_3NH_2$ experiment, most peaks are substantially smaller in the deuterated experiments. However, the absorptions at 2094.3, 2020.6, and 1836.4 cm^{-1} remain virtually unchanged regardless of deuterium enrichment. These peaks, then, correspond to species without amine hydrogens.

$^{nat}B + CH_3ND_2$. Because the gas sample used in this experiment was the same as in the previous experiments with ^{10}B, the hydrogen isotopic multiplets of corresponding peaks are the same and analogous bands were observed as listed in Table 1. Figure 3b presents the best such experiment for this isotopic combination. Note that the intensities of the absorptions at 1830.5, 1981.1, and 2092.3 cm^{-1} are independent of deuterium enrichment, indicating not only that the species lack amine hydrogens but also that these ^{11}B peaks correspond to ^{10}B peaks that have the same intensity as in the CH_3NH_2 experiments.

$B + (CH_3)_2NH$. Several of the absorptions observed in these experiments were observed in the $B + CH_3NH_2$ experiments reported above but at lower intensities. Absent from these spectra are bands from BNBH and HBNH. One prominent new doublet in the $^{10}B + (CH_3)_2NH$ experiment at 2112.5 and 2111.5 cm^{-1} increases 10% on photolysis. Absorptions at 2060.1 and 2058.9 cm^{-1} increase 10% upon photolysis in the corresponding ^{nat}B experiment and represent the same species as the doublet from the ^{10}B experiment.

$B + (CH_3)_3N$. A few experiments involving trimethylamine yielded none of the peaks reported above for monomethylamine. Only a small trace of the doublets at 2112.5, 2111.5 cm^{-1} and 2060.1, 2058.9 cm^{-1} observed in the dimethylamine experiments appeared.

Calculations. Because $^{13}CH_3NH_2$, $CH_3{}^{15}NH_2$, and CD_3NH_2 were not available, identification of species via isotopic shifts of the carbon, nitrogen, and methyl hydrogen atoms was not possible. Instead, Hartree−Fock calculations played a large role in the assignment of the bands. In general, these calculations overestimate vibrational frequencies, but with the MP2 method and D95* basis set, these errors are typically within 5% for closed-shell species. Also, the ratios of vibrational frequencies of corresponding modes with different boron isotopes provide a partial description of the normal mode for comparison with experimental values. Table 2 presents results of several MP2 calculations. This table contains several possible products generated following boron insertion into the N−H, C−H, and C−N bonds and includes several species not observed in the experiments. Because most of these species contain several atoms, they also have several vibrational modes and a complete list of these modes would be quite cumbersome. Table 2, therefore, lists only those modes with intensities above a threshold of 30 km/mol.

Discussion

Identification of products makes use of isotopic shifts in vibrational frequency, involving both boron and hydrogen, combined with MP2 calculations of isotopic frequencies.

Species 1: CH_3BNH. In Figure 2, the 2001.3 and 1940.2 cm^{-1} bands in CH_3NH_2 experiments are assigned to the ^{10}B and ^{11}B counterparts, respectively, of CH_3BNH. Calculations predict this molecule to be the most stable of the $BCNH_4$ isomeric variants (Table 2). The boron isotopic ratio, 1.031 49, actually exceeds the B−N diatomic ratio, 1.027 62. MP2 calculations on this molecule yield corresponding vibrational frequencies of 2068.5 (3.3% higher than experiment) and 2003.6 cm^{-1} (also 3.3% higher than experiment), giving a harmonic isotopic frequency ratio of 1.032 39, in excellent agreement with experiment. The slight discrepancy is in part because of anharmonicity in the observed frequencies. In experiments with CH_3ND_2, which included residual CH_3NH_2 and CH_3NHD, CH_3BND peaks at 1950.7 and 1892.2 cm^{-1} (boron isotopic ratio of 1.030 92) complement much weaker absorptions at 2001.3 and 1940.2 cm^{-1}. The hydrogen isotopic ratios are 1.025 94 and 1.025 37 for ^{10}B and ^{11}B, respectively. The MP2 calculations yield frequencies at 2012.4 (+3.2%) and 1950.0 cm^{-1} (+3.1%) and a boron isotopic ratio of 1.032 00 for CH_3BND. The calculated hydrogen isotopic ratios are 1.027 88 and 1.027 49 for ^{10}B and ^{11}B, respectively. Small hydrogen isotopic shifts indicate little hydrogen coupling to the B−N stretching mode.

Because CH_3BNH resembles HBNH with the boron hydrogen replaced by a methyl group, the N−H stretching frequencies of these molecules should be similar. The absorptions at 3691.1 and 3690.5 cm^{-1} correspond to the two boron isomers of the N−H stretch of CH_3BNH. The photolysis behavior (+40%) matches that of the B−N stretching mode. MP2 calculations yield frequencies of 3886.7 and 3886.3 cm^{-1} (235 and 237 km/mol intensity) with an isotopic ratio of 1.000 10, in very good agreement with the observed ratio of 1.000 16. Although these calculations predict another mode at 482.4 cm^{-1} (140 × 2 km/mol) for both ^{10}B and ^{11}B, only peaks due to HNC and HBNH are observed in this region. The relatively low signal-to-noise ratio in this region of the spectrum makes observation of such low-frequency absorptions difficult.

TABLE 2: SCF Energies, Geometries, and Vibrational Frequencies for H/B/C/N Species Calculated Using the MP2 Method with D95* Basis Set[a]

species	energy (au)	bond lengths (Å)	bond angles (deg)	selected vibrational frequencies (intensities) for natural isotopes [cm^{-1} and km/mol]
CH_3BNCH_3	−158.401 94	$r_{CN} = 1.42$, $r_{BN} = 1.26$, $r_{BC} = 1.55$, $r_{CH} = 1.10$[b]	$\angle_{BCN} = 180.0$, $\angle_{CBN} = 180.0$, $\angle_{BNC} = 180.0$, $\angle_{HNC} = 110.6$, $\angle_{HBC} = 110.8$, $\angle_{HCH} = 108.1,108.3$	3069.0 (74), 2108.9 (212), 1499.6 (30)
$(CH_3)_2NB$	−158.314 78	$r_{BN} = 1.39$, $r_{CN} = 1.47$, $r_{CH} = 1.10$a	$\angle_{BNC} = 121.8$, $\angle_{CNC} = 116.4$, $\angle_{HCN} = 109.5,110.1$, $\angle_{HCH} = 108.9, 109.3$	3166.5 (40), 3070.0 (33), 3068.8 (45), 1587.2 (85), 1479.1 (91), 1133.7 (74)
CH_3BNH	−119.365 72	$r_{CB} = 1.55$, $r_{CH} = 1.10$, $r_{BN} = 1.26$, $r_{NH} = 1.00$	$\angle_{HCB} = 110.6$, $\angle_{HCH} = 108.3$, $\angle_{CBN} = 180.0$, $\angle_{BNH} = 180.0$	3886.3 (235), 2003.6 (138), 482.4 (140 × 2)
CH_3NBH	−119.341 90	$r_{CN} = 1.42$, $r_{CH} = 1.10$, $r_{BN} = 1.26$, $r_{BH} = 1.17$	$\angle_{HCN} = 110.4$, $\angle_{HCH} = 108.6$, $\angle_{CNB} = 180.0$, $\angle_{NBH} = 180.0$	3076.0 (54), 1957.6 (57)
CH_2NBH_2	−119.332 04	$r_{CH} = 1.10$, $r_{CN} = 1.26$, $r_{NB} = 1.37$, $r_{BH} = 1.19$	$\angle_{HCN} = 121.2$, $\angle_{HCH} = 117.6$, $\angle_{CNB} = 180.0$, $\angle_{NBH} = 117.8$, $\angle_{HBH} = 124.3$	3105.4 (49), 2751.6 (105), 2648.4 (90), 1922.1 (74), 1051.5 (32)
CH_2BNH_2	−119.331 01	$r_{CB} = 1.40$, $r_{CH} = 1.09$, $r_{BN} = 1.38$, $r_{NH} = 1.01$	$\angle_{HCB} = 121.7$, $\angle_{HCH} = 116.5$, $\angle_{CBN} = 180.0$, $\angle_{BNH} = 122.6$, $\angle_{HNH} = 114.7$	3729.5 (76), 3621.0 (67), 1822.3 (282), 682.9 (106), 489.6 (255)
BH_2CHNH	−119.291 57	$r_{BC} = 1.57$, $r_{BH} = 1.19$[a], $r_{CN} = 1.31$, $r_{CH} = 1.10$, $r_{NH} = 1.03$	$\angle_{HBC} = 121.2$, $\angle_{HBH} = 117.9, 120.8$, $\angle_{CBN} = 180.0$, $\angle_{BNH} = 180.0$	2766.0 (118), 2658.9 (86), 1278.4 (48), 1259.4 (54), 1204.0 (56), 655.9 (34)
$BHCHNH_2$	−119.246 21	$r_{CN} = 1.47$, $r_{BC} = 1.41$, $r_{CH} = 1.09$, $r_{BH} = 1.17$, $r_{NH} = 1.02$	$\angle_{BCN} = 125.3$, $\angle_{BCH} = 120.0$, $\angle_{HBC} = 180.0$, $\angle_{CNH} = 110.4$, $\angle_{HNH} = 107.6$	1691.7 (33), 877.4 (93), 832.1 (36), 706.5 (60)
CH_2BNH	−118.739 39	$r_{CB} = 1.51$, $r_{CH} = 1.09$, $r_{BN} = 1.26$, $r_{NH} = 1.00$	$\angle_{HCB} = 121.7$, $\angle_{HCH} = 116.6$, $\angle_{CBN} = 180.0$, $\angle_{BNH} = 180.0$	3890.3 (277), 2072.6 (332), 503.0 (140), 433.3 (152)
CH_2NBH	−118.725 85	$r_{CN} = 1.35$, $r_{CH} = 1.09$, $r_{NB} = 1.26$, $r_{BH} = 1.17$	$\angle_{HCN} = 119.4$, $\angle_{HCH} = 121.3$, $\angle_{CNB} = 180.0$, $\angle_{NBH} = 180.0$	2998.2 (67), 2042.5 (329), 321.6 (92)
CH_3NB	−118.697 63	$r_{CN} = 1.42$, $r_{CH} = 1.10$, $r_{BN} = 1.24$	$\angle_{HCN} = 110.5$, $\angle_{HCH} = 108.4$, $\angle_{CNB} = 180.0$	3074.4 (401), 2251.5 (759)
CH_3BN	−118.669 65	$r_{CB} = 1.55$, $r_{CH} = 1.10$, $r_{BN} = 1.26$	$\angle_{HCB} = 110.3$, $\angle_{HCH} = 108.6$, $\angle_{CBN} = 180.0$	2049.9 (530)
BH_2NC	−118.162 26	$r_{BH} = 1.19$, $r_{BN} = 1.44$, $r_{NC} = 1.20$	$\angle_{HBN} = 117.5$, $\angle_{HBH} = 124.9$, $\angle_{BNC} = 180.0$	2828.0 (92), 2701.9 (102), 2115.4 (288), 1266.9 (86), 1081.0 (48), 982.4 (61)
BH_2CN	−118.153 35	$r_{BC} = 1.55$, $r_{BH} = 1.19$, $r_{CN} = 1.19$	$\angle_{HBC} = 118.5$, $\angle_{HBH} = 123.0$, $\angle_{BCN} = 180.0$	2825.3 (73), 2705.9 (74), 2177.3 (54), 1239.3 (47), 1056.1 (43), 874.7 (45)
CH_2NB	−118.081 30	$r_{CH} = 1.10$, $r_{CN} = 1.27$, $r_{NB} = 1.39$	$\angle_{HCN} = 121.4$, $\angle_{HCH} = 117.3$, $\angle_{CNB} = 180.0$	3096.6 (57), 1901.4 (440), 1054.3 (90)
HBCNH	−118.053 22	$r_{CB} = 1.39$, $r_{CN} = 1.27$, $r_{BH} = 1.17$, $r_{NH} = 1.03$	$\angle_{BCN} = 180.0$, $\angle_{HBC} = 183.4$, $\angle_{CNH} = 111.1$	1187.4 (154), 816.5 (50), 474.4 (35)
CH_2BN	−118.036 20	$r_{CH} = 1.09$, $r_{CB} = 1.49$, $r_{BN} = 1.28$	$\angle_{HCB} = 121.9$, $\angle_{HCH} = 116.1$, $\angle_{CBN} = 180.0$	918.2 (35)

[a] Only those vibrational frequencies with calculated intensities of at least 30 km/mol are shown [b] Inequivalent bonds.

This molecule resembles isoelectronic methylacetylene, CH_3CCH. In CH_3BNH, a B−N triple bond replaces the C−C triple bond of methylacetylene. Addition of a methyl group to acetylene increases the C−C stretching frequency from 1974 cm^{-1} to 2142 cm^{-1} in the gas phase.[22] Addition of a methyl group to the boron atom of HBNH increases the B−N stretching frequency, in the ^{11}B case, from 1782.7 and 1788.1 cm^{-1} to 1940.2 cm^{-1}, a comparable increase of 155 ± 3 cm^{-1}. This increase in vibrational frequency upon methylation underscores the similarity between the C−C and B−N triple bonds.

Species 2: CH_3NBH. In Figure 2, the absorptions at 1975.5 and 1949.2 cm^{-1} are assigned to CH_3NBH for ^{10}B and ^{11}B, respectively. The deuterated counterparts in Figure 3 appear at 1753.5 and 1749.2 cm^{-1}. Table 2 shows a calculated energy for CH_3NBH only 15 kcal/mol higher than that of CH_3BNH, indicating the possibility of observing both methyliminoboranes. MP2 calculations generate ^{10}B and ^{11}B frequencies of 1985.3 (+0.5%) and 1957.6 cm^{-1} (+0.4%) for the CH_3NH_2 reaction. The calculated isotopic ratio of 1.014 15 compares favorably with the experimental value of 1.013 49. For CH_3NBD, the corresponding calculated frequencies are 1803.7 (+2.9%) and 1798.5 cm^{-1} (+2.8%) with a boron isotopic ratio of 1.002 89 (versus 1.002 46 for experiment). The observed hydrogen isotopic ratio shifts, 1.126 60 for ^{10}B and 1.114 34 for ^{11}B, agree very well with the respective calculated shifts of 1.100 68 and 1.088 46. The small boron isotopic shift in the deuterated molecule arises from coupling between the similarly energetic B−N and B−D modes in this molecule.

Note also that this species, like CH_3BNH, is analogous to methylacetylene, except that the addition of the methyl group occurs on the nitrogen. That the increase in vibrational frequency, from 1782.7 and 1788.1 cm^{-1} to 1949.2 cm^{-1}, also compares with that of methylacetylene further confirms the similarity of the iminoboranes with methylacetylene.

Species 3: CH_2BNH_2. The absorptions at 1798.5 and 1743.5 cm^{-1} in the B + CH_3NH_2 spectra (Figure 2) correspond to CH_2BNH_2, only 22 kcal/mol higher in energy than CH_3BNH. The methylene and amine hydrogens lie in planes orthogonal to each other with boron double bonded to both carbon and nitrogen, according to the calculations. The observed boron isotopic ratio of 1.031 55 exceeds the B−N diatomic ratio and indicates a mode similar to that of CH_3BNH, in which the boron vibrates between carbon and nitrogen. MP2 calculations predict vibrational frequencies of 1881.5 (+4.6%) and 1822.3 cm^{-1} (+4.5%) with a boron isotopic ratio of 1.032 49, in excellent agreement with the observed ratio.

Spectra of experiments with CH_3ND_2, which included ample monodeuterated and nondeuterated species, exhibited hydrogen isotopic triplets in this region (Figure 3). For ^{10}B, the triplet at 1798.5, 1794.1, and 1786.2 cm^{-1} matches the triplet at 1743.5,

1741.1, and 1734.8 cm^{-1} for ^{11}B with corresponding boron isotopic ratios of 1.031 55, 1.030 44, and 1.029 63, respectively. The hydrogen isotopic ratios are 1.00689:1.00442:1.0 for ^{10}B and 1.00501:1.00363:1.0 for ^{11}B. MP2 calculations predict vibrational frequencies of 1875.9 (+4.6%), 1870.6 (+4.7%), 1815.3 (+4.3%), and 1809.8 cm^{-1} (+4.3%) for $CH_2{}^{10}BNHD$, $CH_2{}^{10}BND_2$, $CH_2{}^{11}BNHD$, and $CH_2{}^{11}BND_2$, respectively. The calculated boron isotopic ratios, 1.033 38 for CH_2BNHD and 1.033 59 for CH_2BND_2, agree well with experiment as do the hydrogen isotopic ratios, 1.00583:1.00283:1.0 for ^{10}B and 1.00691:1.00304:1.0 for ^{11}B. The employment of partially deuterated CH_3ND_2 enabled both the presence of these hydrogen isotopic triplets and the subsequent identification of CH_2BNH_2 as the only major reaction product with two amine hydrogens.

Species 4: CH_3BNCH_3. Because CH_3NH_2 contains only one methyl group and $(CH_3)_2NH$ contains two, only in reactions of boron with the latter should the dimethyliminoborane be formed. Absorptions at 2112.5, 2111.5 cm^{-1} and 2060.1, 2058.9 cm^{-1} in the B + $(CH_3)_2NH$ experiments do not appear in the B + CH_3NH_2 experiments and are assigned to CH_3BNCH_3. The boron isotopic ratios, 1.025 44 and 1.025 55, are nearly that of the B−N diatomic. MP2 calculations predict corresponding absorptions at 2163.6 (+2.4%) and 2108.9 cm^{-1} (+2.4%) and a boron isotopic ratio of 1.025 94, in excellent agreement with experiment. In experiments with deuterium-passivated environments (i.e., some $(CH_3)_2ND$ in the gas sample), the absence of a deuterium shift confirms this assignment. CH_3BNCH_3 is also calculated to be 55 kcal/mol more stable than its isomeric variant, $(CH_3)_2NB$, which has a terminal boron atom.

CH_3BNCH_3, like CH_3BNH and CH_3NBH, also has an isoelectronic acetylene analogue, dimethylacetylene, CH_3CCCH_3. Addition of a methyl group to CH_3BNH or CH_3NBH increases the B−N stretching frequency by 112 or 119 cm^{-1}. Addition of a second methyl group to methylacetylene increases the C−C vibrational frequency from 2142 to 2313 cm^{-1}, an increase larger than the one observed for the B−N stretch of the iminoboranes.[22] Nevertheless, the frequencies of both the C−C and B−N bonds increase significantly upon further methylation.

Species 5: CH_3NB. The absorptions at 2020.6 and 1981.1 cm^{-1} are weaker than those of species **1**−**3** and do not show any deuterium isotope shift. The isotopic ratio, 1.019 94, is less than that of diatomic BN and resembles more that of CH_3NBH, in which the B−N mode couples somewhat with the B−H vibration, than those of CH_3BNH and CH_2BNH_2, in which coupling between the B−N and N−H modes is small. Therefore, the likely species corresponding to these peaks is the radical CH_3NB. Although MP2 calculations work better for closed-shell molecules than for open-shell radicals, the predictions for CH_3NB agree reasonably well with the assignment. The calculated B−N stretching frequencies, predicted at 2302.4 (+13.9%) and 2251.5 cm^{-1} (+13.6%) for ^{10}B and ^{11}B, are more than 1 order of magnitude more intense than any other mode in the radical. The calculated intensity of 759 km/mol (for $CH_3N^{11}B$) indicates that the observation of these absorptions may owe less to a substantial yield than to a strong oscillator strength for the B−N vibrational mode. Although the calculations predict frequencies that exceed the experimental frequencies by more than in the closed-shell cases, the boron isotopic ratio, 1.022 61, agrees reasonably well with the observed ratio. According to Table 2, MP2 calculations predict this species to be more stable than its isomeric variant, CH_3BN, by 18 kcal/mol, and the boron isotopic shift of CH_3BN (1.031 46) does not agree with the experimental results for these absorptions.

Species 6: CH_2BNH. The absorptions at 1939.3 and 1881.0 cm^{-1} track with each other well. No obvious 4:1 doublet appears because the strong CH_3BNH peak at 1940.2 cm^{-1} obscures the weak absorption on its shoulder at 1939.3 cm^{-1}. These peaks recede considerably in the deuterated amine work and denote a species with one amine hydrogen. Because of its relative calculated stability (26 kcal/mol more stable than CH_3NB) and its positioning of boron between the carbon and nitrogen, we suggest CH_2BNH radical as this product. The large boron isotopic ratio, 1.030 99, suggests boron bonded between carbon and nitrogen, as in CH_3BNH. MP2 calculations predict frequencies of 2140.6 (+10.4%) and 2072.6 cm^{-1} (+10.2%) for the B−N stretching mode, an isotopic ratio of 1.032 81. Because this species is an open-shell radical, the predictions of the calculations differ from experiment by a greater margin than for the closed-shell molecules, but the boron isotopic shift closely resembles that of experiment.

For its deuterated counterpart, the peaks at 1895.5 and 1839.4 cm^{-1} fit well for ^{10}B and ^{11}B, respectively. In the ^{nat}B experiment with CH_3ND_2, a shoulder of the intense 1892.2 cm^{-1} peak has sufficient intensity to indicate that a small absorption at 1895.5 cm^{-1} exists. The hydrogen isotopic ratios are 1.023 11 and 1.022 62 for ^{10}B and ^{11}B, and the boron isotopic ratio is 1.030 50. Calculations give frequencies of 2079.8 (+9.7%) and 2015.5 cm^{-1} (+9.6%) for ^{10}B and ^{11}B, with a boron isotopic ratio of 1.031 90, in good agreement with experiment. The calculated hydrogen isotopic ratios of 1.029 23 (^{10}B) and 1.028 33 (^{11}B) also agree with the results reported here.

Species 7: CH_2NB. The absorptions at 1836.5 and 1830.5 cm^{-1} for ^{10}B and ^{11}B, respectively, do not shift upon amine deuteration, indicating that these peaks correspond to a product without amine hydrogens. On the basis of the MP2 calculations, the most likely identity for this species is CH_2NB. These calculations predict absorptions at 1908.1 (+3.9%) and 1901.4 cm^{-1} (+3.9%) for ^{10}B and ^{11}B. The calculated boron isotopic ratio (1.003 52) closely matches that of experiment (1.003 28). The strong calculated intensities (457 and 440 km/mol) for these relatively small absorptions indicate that this species may only be a minor product. Although other similar species, like BH_2CN, are calculated to be more stable thermodynamically, preferential formation of CH_2NB may occur because of a more favorable reaction mechanism.

Species 8: BH_2CN. The absorptions at 2094.3 and 2092.2 cm^{-1} for ^{10}B and ^{11}B, respectively, track well on photolysis and are assigned to the same product. Because the boron shift is so small, this absorption most likely corresponds to a C−N triple bond vibration as opposed to a B−N triple bond vibration. Also, these absorptions lose no intensity in the deuterated experiments, indicating no amine hydrogens. On the basis of this information and the MP2 calculations, the most likely candidate for this molecule is BH_2CN. The calculated C−N stretches occur at 2178.7 (+4.0%) and 2177.3 cm^{-1} (+4.1%) for the two boron isotopes. Although this molecule should be slightly less stable than the isomeric variant BH_2NC, the latter may not be formed because of the stability of the alternatives. That is, because N−H insertion yields many stable products under the experimental conditions, BH_2NC may not be competitive. However, because few products exist for C−H insertion, BH_2CN may be quite stable relative to other products that could be formed in this manner. Also, the large increase in peak size upon photolysis and the corresponding decrease in size for BCN absorptions could indicate a process by which BCN situated near a H_2 molecule reacts to form BH_2CN. Although the information in Table 2 suggests that several other absorbances of this molecule should be of nearly the same intensity as the

SCHEME 1

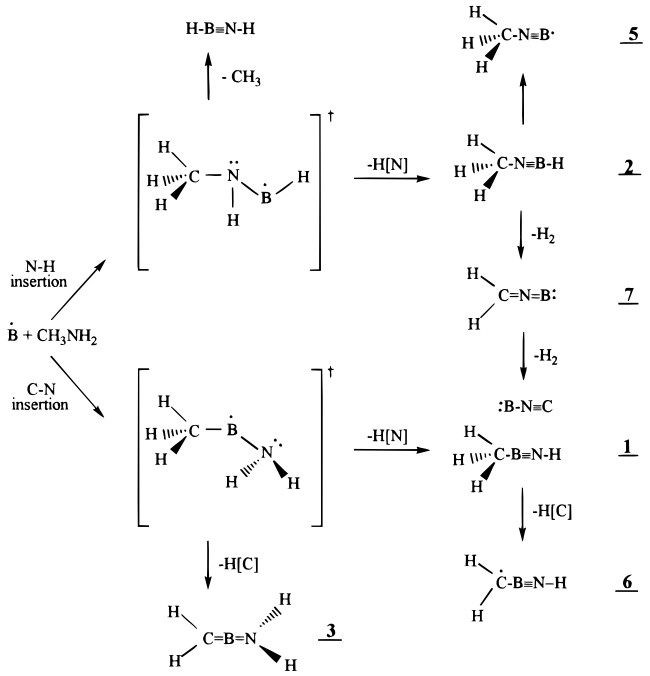

C−N stretch, no other peak from this molecule is observed. Nevertheless, the calculated intensities may underestimate the relative strength of the C−N absorption, as for BCN and BNC.[21]

Reaction Mechanisms. The excess kinetic energy imparted to the boron atoms in the ablation process[23] allows for the formation of several different products. Reactions of boron with mono- and dimethylamine proceed via insertion into one of three possible bonds: the C−H bond, the N−H bond, and the C−N bond. In the first case, such reactions should behave similarly to those of the boron reactions with methane and yield similar products. In the second case, reaction products should resemble those of the boron−ammonia reactions. C−N insertion is unique to the experiments reported here. Because the dominant spectroscopic features of the products in these experiments occur in the B−N stretching region, the evidence suggests that insertion into the N−H or C−N bonds is much more favorable than insertion into the C−H bond. The observation of BH_2CN and a trace of HBCBH[6] shows that some C−H insertion does occur, but C−H insertion makes only a minor contribution to the overall reaction mechanism. Scheme 1 presents mechanisms involving N−H and C−N insertion.

MP2 calculations on the insertion products for all three potential mechanisms reveal that the N−H and C−N insertions are energetically favored over C−H insertion. Insertion into the N−H bond to make CH_3NHBH is exoergic by 86 kcal/mol, while insertion into the C−N bond to make CH_3BNH_2 is exoergic by 79 kcal/mol. By contrast, insertion into the C−H bond to make $HBCH_2NH_2$ is exoergic by only 48 kcal/mol; thermodynamics favor C−N and N−H insertion over C−H insertion, in agreement with the product spectra.

For insertion into the N−H bond, products might form by losing either a methyl group or a hydrogen. If in the monomethylamine reactions methyl elimination follows boron insertion, the spectra would show absorptions of products similar to those observed in the boron−ammonia reactions. This mechanism accounts for the presence of HBNH and BNBH in the spectra. Although reactions of boron with ammonia generated in the laser plume may spawn some of these products, the small concentration of matrix-isolated ammonia relative to that of the parent monomethylamine indicates that boron−ammonia reactions cannot produce a significant amount of product in these experiments. Similarly, if in the dimethylamine reaction methyl elimination follows boron insertion into the N−H bond, the spectra would show products similar to those of the monomethylamine reactions. The yield of these products is somewhat lower in the dimethylamine experiments, but the weak absorbance of monomethylamine in the matrix isolation spectrum indicates that dimethylamine reactions primarily form these products. For example, boron insertion into the N−H bond of $(CH_3)_2NH$ followed by methyl elimination would form CH_3NBH.

The reaction mechanism following C−N insertion resembles that of N−H insertion. In the monomethylamine reaction, subsequent elimination of an amine hydrogen generates CH_3BNH, as does elimination of a methyl group in the dimethylamine reaction. C−N insertion followed by elimination of a methyl hydrogen can form CH_2BNH_2, but in the dimethylamine reaction, formation of CH_2BNH_2 entails hydrogen atom migration, a requirement leading to the markedly reduced yield in those experiments. Elimination of the methyl group in the monomethylamine reaction produces HBNH, which shows prominent peaks in the reaction spectra. The absence of HBNH in the dimethylamine reaction results from the absence of a path to that product short of hydrogen rearrangement. Similarly, the absence of two methyl groups in the monomethylamine reaction is responsible for the absence of CH_3BNCH_3. C−N insertion followed by H elimination forms this product in the $(CH_3)_2NH$ reaction.

For the C−H insertion mechanism, the expected products, $HBCHNH_2$, BH_2CHNH, and HBCNH, should generate strong B−C vibrational absorptions near 1500 cm^{-1}. The spectra present no absorptions. Energies of these species from MP2 calculations (Table 2) suggest that these molecules are of significantly higher energy than the observed molecules with B−N bonds. In the B + CH_4 reaction, C−H insertion was the favored pathway to novel products because it was the only pathway available. In the amine reactions, however, far more favored pathways exist and C−H insertion cannot compete with these channels. The main exceptions to this rule are BCN and BH_2CN. Minor HBCBH absorptions, at 1895.2, 1883.9, and 1872.0 cm^{-1} for the different boron isotopic combinations,[6] provide another exception to this rule, and because these absorptions are weak despite a large oscillator strength, HBCBH is not a major product in these experiments.

The major product species observed in these experiments exhibited 1:4 isotopic doublets in the natural boron experiments. In the monomethylamine experiments, BNBH gives rise to the only significant boron isotopic quartet in these experiments and $BNBCH_3$ is not observed. MP2 calculations reveal that if $BNBCH_3$ is formed, there must be strong absorptions in the B−N stretching region. Barring H migration, the formation of $BNBCH_3$ would most likely occur from insertion into the C−N bond of CH_3NBH followed by H elimination or insertion into the N−H bond of CH_3BNH followed by H elimination. BNBH forms in this experiment by CH_3 elimination following either C−N insertion into CH_3NBH or N−H insertion into CH_3BNH. Therefore, CH_3 elimination must be much more favored following secondary boron insertion into CH_3NBH or CH_3BNH.

Conclusions

The study of the reactions of boron with mono- and dimethylamine complement the previous boron−ammonia work in this laboratory and give rise to the detection of new iminoboranes and other related species. Two classes of mechanisms can account for the products. The first, involving

insertion into the N−H bond, parallels the dominant mechanism of the ammonia reactions. The second mechanism, involving insertion into the C−N bond, enables the formation of many of the species reported here. A third possible mechanism involving insertion into the C−H bond parallels the mechanism for the B + CH_4 reaction but cannot compete with the alternatives in these experiments.

Acknowledgment. The experimental work was supported by the Air Force Office of Scientific Research, and calculations were done at the San Diego Supercomputer Center.

References and Notes

(1) Burkholder, T. R.; Andrews, L. *J. Chem. Phys.* **1991**, *95*, 8697.
(2) Andrews, L.; Burkholder, T. R. *J. Phys. Chem.* **1991**, *95*, 8554.
(3) Hassanzadeh, P.; Andrews, L. *J. Phys. Chem*. **1992**, *96*, 9177.
(4) Andrews, L.; Hassanzadeh, P.; Burkholder, T. R.; Martin, J. M. L. *J. Chem. Phys.* **1993**, *98*, 922.
(5) Tague, T. J., Jr.; Andrews, L. *J. Am. Chem. Soc.* **1994**, *116*, 4970.
(6) Hassanzadeh, P.; Andrews, L. *J. Am. Chem. Soc.* **1992**, *114*, 9239.
(7) Hassanzadeh, P.; Hannachi, Y.; Andrews, L. *J. Phys. Chem.* **1993**, *97*, 6418.
(8) Thompson, C. A.; Andrews, L. *J. Am. Chem. Soc.* **1995**, *117*, 10125.
(9) Thompson, C. A.; Andrews, L.; Martin, J. M. L.; El-Yazal, J. *J. Phys. Chem.* **1995**, *99*, 13839.
(10) Lory, E.; Porter, R. *J. Am. Chem. Soc.* **1973**, *95*, 1767.
(11) Kawashima Y.; Kawaguchi, K.; Hirota, E. *J. Chem. Phys*. **1987**, *87*, 6331.
(12) Frisch, M. J.; Trucks, G. W.; Schlegel, H. B.; Gill, P. M. W.; Johnson, B. G.; Robb, M. A.; Cheeseman, J. R.; Keith, T.; Petersson, G. A.; Montgomery, J. A.; Raghavachari, K.; Al-Laham, M. A.; Zakrzewski, V. G.; Ortiz, J. V.; Foresman, J. B.; Cioslowski, J.; Stefanov, B. B.; Nanayakkara, A.; Challacombe, M.; Peng, C. Y.; Ayala, P. Y.; Chen, W.; Wong, M. W.; Andres, J. L.; Replogle, E. S.; Gomperts, R.; Martin, R. L.; Fox, D. J.; Binkley, J. S.; Defrees, D. J.; Baker, J.; Stewart, J. P.; Head-Gordon, M.; Gonzalez, C.; Pople, J. A. *Gaussian 94*, Revision B.1; Gaussian, Inc.: Pittsburgh, PA, 1995.
(13) Head-Gordon, M.; Pople. J. A.; Frisch, M. J. *Chem. Phys. Lett.* **1988**, *153*, 503. Frisch, M. J.; Head-Gordon, M.; Pople, J. A. *Chem. Phys. Lett.* **1990**, *166*, 275. Frisch, M. J.; Head-Gordon, M.; Pople, J. A. *Chem. Phys. Lett.* **1990**, *166*, 281.
(14) Dunning, T. H., Jr.; Hay, P. J. In *Modern Theoretical Chemistry*; Schaefer, H. F., III, Ed.; Plenum: New York, 1976; pp 1−28.
(15) Schlegel, H. B. *J. Comput. Chem.* **1982**, *3*, 214.
(16) Jacox, M. E.; Milligan, D. E. *J. Mol. Spectrosc.* **1975**, *56*, 333.
(17) Milligan, D. E.; Jacox, M. E. *J. Chem. Phys.* **1967**, *47*, 278.
(18) Bohn, R. B.; Andrews, L. *J. Phys. Chem.* **1989**, *93*, 3974.
(19) Milligan, D. E.; Jacox, M. E. *J. Chem. Phys.* **1967**, *47*, 5146.
(20) Hinze, J.; Curl, R. J., Jr. *J. Am. Chem. Soc.* **1964**, *86*, 5068. Stolkin, I.; Ha, T.-K.; Gunthard, H. H. *Chem. Phys.* **1977**, *21*, 327. Machara, N. P.; Ault, B. S. *Chem. Phys. Lett.* **1987**, *140*, 411.
(21) Lanzisera, D. V.; Andrews, L. Unpublished.
(22) Boyd, D. R. J.; Thompson, H. W. *Trans. Faraday Soc.* **1952**, *48*, 493. Herzberg, G. *Infrared and Raman Spectra of Polyatomic Molecules*; Van Nostrand: New York, 1945.
(23) Kang, H.; Beauchamp, J. L. *J. Phys. Chem.* **1985**, *89*, 3364.